JOURNAL OF MATERIALS SCIENCE **36** (2001) 3885–3890

High resolution microscopy study in Cr_3C_2-doped WC-Co

T. YAMAMOTO, Y. IKUHARA, T. WATANABE
Engineering Research Institute, The University of Tokyo, 2-11-16, Yayoi, Bunkyo-ku, Tokyo 113-8656, Japan
E-mail: yamamoto@sogo.t.u-tokyo.ac.jp

T. SAKUMA
Department of Advanced Materials Science, The University of Tokyo, 7-3-1, Hongo, Bunkyo-ku, Tokyo 113-8656, Japan

Y. TANIUCHI, K. OKADA, T. TANASE
Central Research Institute, Mitsubishi Materials Corp., 1-297 Kitabukuro-cho, Omiya, Saitama 330, Japan

Microstructure in Cr_3C_2-doped WC-Co was examined by high-resolution electron microscopy (HRTEM) and X-ray energy dispersive spectroscopy (EDS) with a special interest in the segregation of Cr at WC/Co interfaces and WC/WC grain boundaries. The macroscopic morphology of carbide grains in Cr_3C_2-doped WC-Co was almost the same as that of non-doped one, however, doping of a small amount of Cr_3C_2 on WC-Co was found to be effective to reduce the grain size of carbide grains. HRTEM study revealed that both WC/Co and WC/WC interfaces were free from secondary phases or amorphous films. Nano-probe EDS analysis revealed that Cr segregated at both WC/Co and WC/WC interfaces in the Cr_3C_2 doped WC-Co. The grain growth retardation of carbide grains observed in the Cr_3C_2-doped WC-Co must be closely related to the segregation of Cr. On the other hand, an asymmetric tilt $\Sigma 2$ grain boundary of WC/WC was observed in the grain orientation of $(0001)//(11\bar{2}0)$, $[1\bar{2}10]//[\bar{1}101]$. The formation of this coherent boundary results from a small misfit of about 2% in a/c-axis of WC hexagonal lattice structure. The segregation of Cr and Co was detected also at this boundary in spite of high coherent boundary. This would be due to a small distortion of the grain boundary from an ideal $\Sigma 2$ boundary.

1. Introduction

WC-Co based cemented carbides are often used as cutting tools or mechanical drills since they have high hardness and high wear resistance [1]. It is well known that the mechanical properties can be improved by the reduction of a grain size of carbides. For this purpose, transition metal carbides such as VC, TaC and Cr_3C_2 are often doped in WC-Co based compounds [2, 3]. However, the role of the transition metal carbides as inhibitors for the grain growth is not cleared yet. Recently our group has performed high-resolution transmission electron microscopy (HRTEM) analysis for VC-doped WC-Co compounds. As a result, the morphology change of WC/Co interfaces was revealed, i.e., from ordinary faceting feature in non-doped compounds to fine multi-step shape in VC-doped ones. In addition, the formation of $(W, V)_2C$ compounds were confirmed at WC/Co interfaces in the doped compound at an atomic scale [4, 5]. Namely, the inhibition of WC grain growth caused by VC-doping is considered to be due to the formation of $(W, V)_2C$ compounds along the interfaces of WC/Co. On the other hand, Cr_3C_2 is also known to be one of the inhibitors for the carbide grain growth [6]. However, there have been few studies to characterize the interface structures from the viewpoint of atomic scale analysis as mentioned above.

In this study, microstructural analysis was performed for Cr_3C_2-doped WC-Co by high-resolution transmission electron microscopy (HRTEM) and X-ray energy dispersive spectroscopy (EDS) with highly spatial resolution in order to clarify the structure of WC/Co interfaces and WC/WC grain boundaries

2. Experimental procedure

WC powders of an average grain size of 0.8 μm (Japan New Metals Co Ltd.), Co powders of 1.2 μm (Stark Co. Ltd.) and Cr_3C_2 powders of 2.3 μm (H. C. Stark Co. Ltd.) were used as raw materials. They were mixed in an attritor-mill for 2 h with the composition of WC-12wt%Co or WC-0.9wt%Cr_3C_2-12wt%Co, respectively. After dried and sieved, the mixtures were compacted under a pressure of 150 MPa. Then the respective green compacts were heated to 1380°C in a

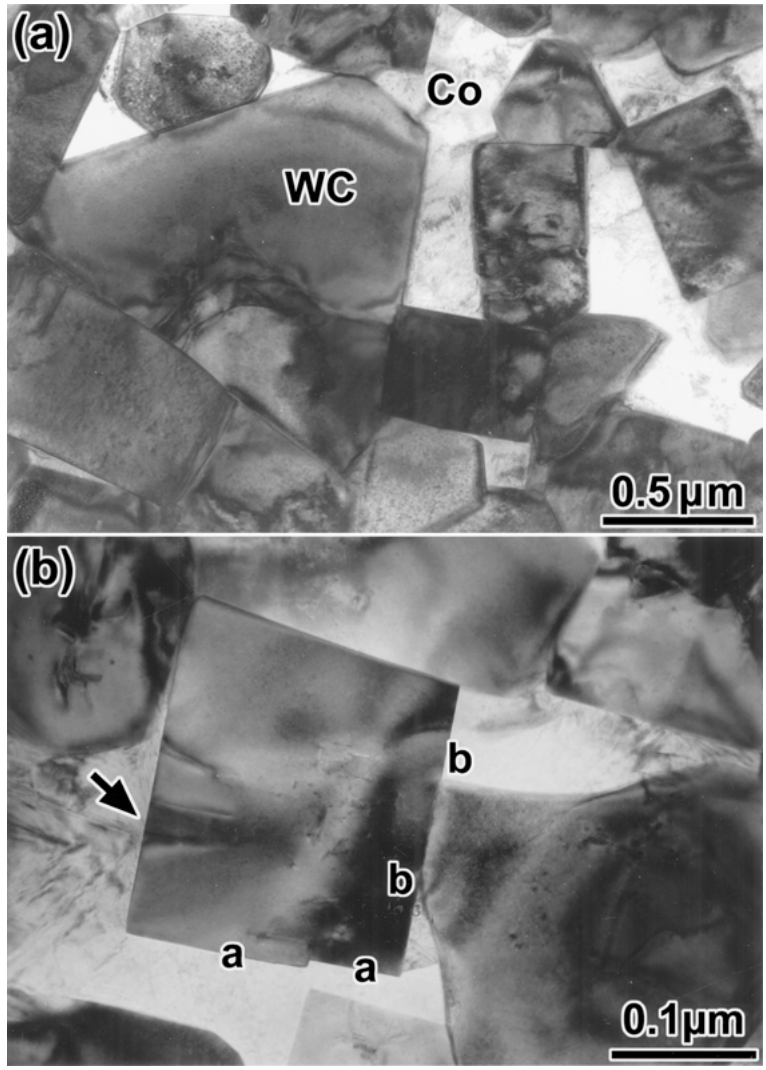

Figure 1 Bright field images in (a) non-doped and (b) Cr-doped compounds in as-sintered state. Note that the magnification is different between the two photographs. Notations in the figure (b) are described in the text.

vacuum at a heating rate of 5°C/min and kept at 1380°C for 1 h. After keeping at the sintering temperature, they were cooled down to room temperature by introducing He gas into the furnace. The approximate cooling rate was more than 50°C/min. Hereafter, these two sintered bodies will be noted as non-doped and Cr-doped compounds, respectively.

Thin foils for HRTEM observation were prepared as follows. Samples with the size of $1 \times 5 \times 15$ mm^3 were machined from the sintered bodies and punched out in a disk shape of ϕ3 mm with an ultra sonic disk cutter. The cut samples were ground to 70 μm thickness and further polished and finished to the mirror state with diamond slurry of 9, 3 and 1 μm. Then, they were dimpled to 20 μm thickness at a center of the disk. After dimpled, these disks were ion-milled (Model 600TMP, Gatan) under a condition of 5 kV $\times$ 1 mA. High-resolution electron microscopy observation was carried out with a HRTEM (H-9000NAR, Hitachi) at an accelerating voltage of 300 kV. Chemical analysis was yielded with an energy dispersive X-ray spectroscope (EDS, Voyager, Noran) equipped to a field-emission type HRTEM (EM-002BF, TOPCON) at 200 kV. An electron probe used for EDS analysis was about ϕ0.5 nm.

3. Results and discussion

Fig. 1 shows bright field images of (a) non-doped and (b) Cr-doped compounds in as-sintered state. In the figure, black and white contrasts correspond to carbide grains and Co phases, respectively. The morphology of carbide grains is not so much different between the two compounds except the grain size of carbide grains. The average grain size of carbides is estimated to be about 0.67 μm in the non-doped compound and 0.4 μm in the Cr-doped one, respectively. This is consistent with the reported result that a small addition of Cr_3C_2 is effective to suppress the grain growth of carbide grains [3, 6]. On the other hand, hardness of the two compounds is estimated to be 1410 HV in the non-doped compound and 1540 HV in the Cr-doped one. The improvement of the hardness is due to the reduction of carbide grains as confirmed in Fig. 1.

High-resolution study was performed for various WC/Co interfaces. All of them were found to be free from any secondary phases. Typical example is shown in Fig. 2. Fig. 2 is a high-resolution image in the vicinity of the WC/Co interface in the Cr-doped compound, which corresponds to the interface as indicated by a-a in Fig. 1b. The areas for EDS analysis are also shown

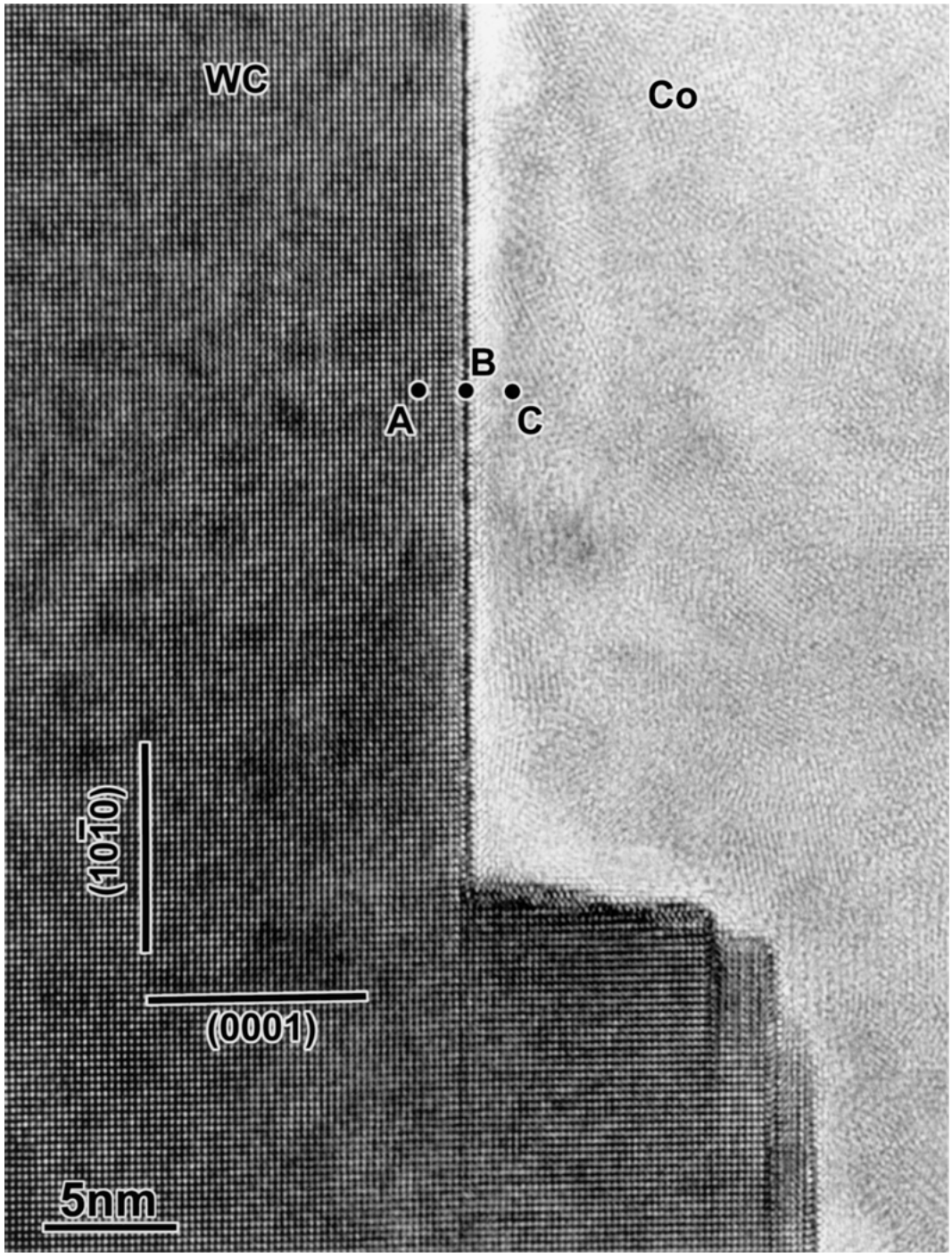

Figure 2 A HRTEM image in the vicinity of WC/Co interface in the Cr-doped compound. Alphabetical indexes correspond to EDS analysis areas.

alphabetically with the dots in the figure. The observed direction is parallel to the [1$\bar{2}$10] of the WC grain and the WC/Co interface is set at the edge-on condition. As seen in the figure, WC/Co interface consists of two kinds of habits. One is (10$\bar{1}$0) plane and the other is the plane nearly parallel to (0001) plane, which correspond to popular habit planes in non-doped WC-Co compounds [7]. There are no any other secondary phases at the interface even in an atomic level. These features are similar to that in non-doped compound.

Fig. 3 shows EDS spectra across the WC/Co interface taken from the areas as indicated in Fig. 2 at an interval of 2 nm. A peak of Cr Kα-line clearly appears in all of the spectra, but the intensity is very different among them. The intensity of the peak from the WC/Co interface is the highest in comparison with the other two spectra. Since there are no secondary phases at the interface, it is considered that the doped Cr segregates at the interface of WC/Co.

Fig. 4 is a plot of element content estimated from EDS analysis in the vicinity of the interface. The analyses were systematically conducted across the interface (10$\bar{1}$0) habit at every several nanometer. The profiles clearly show that Cr segregates at the WC/Co interface over a range of $\sim$4 nm inside WC grain. In addition, Co also diffuses into WC grain in the region of less than 4 nm from the interface.

Transition metal carbides have been often doped in WC-Co-based compounds in order to reduce the size of carbide grains because smaller grain size is suitable for the improvement of mechanical properties [1]. VC is one of the most effective inhibitor for this purpose

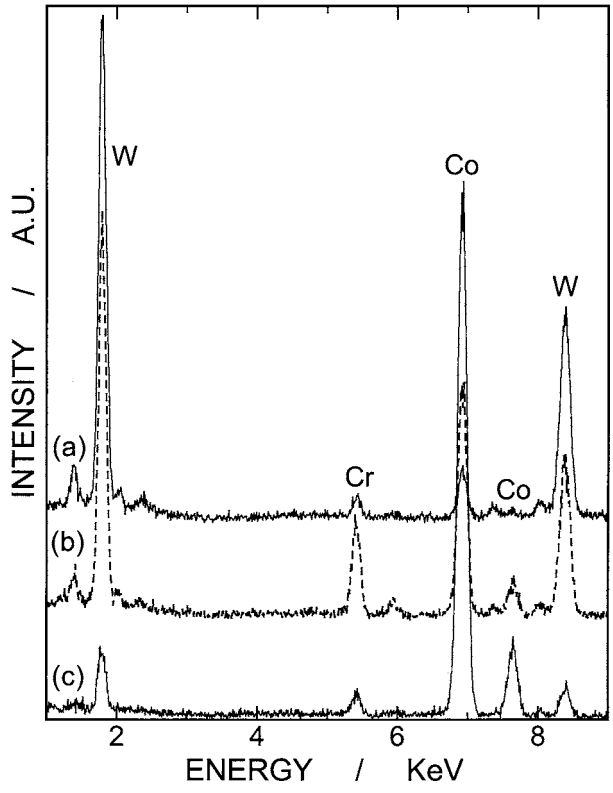

Figure 3 EDS spectra taken from (a) WC grain interior of 2 nm away from the WC/Co interface, (b) WC/Co interface and (c) Co-phase interior of 2 nm away from the interface. The EDS points of (a), (b) and (c) correspond to the areas of A, B and C in Fig. 2, respectively. Note that doped Cr segregates at the interface.

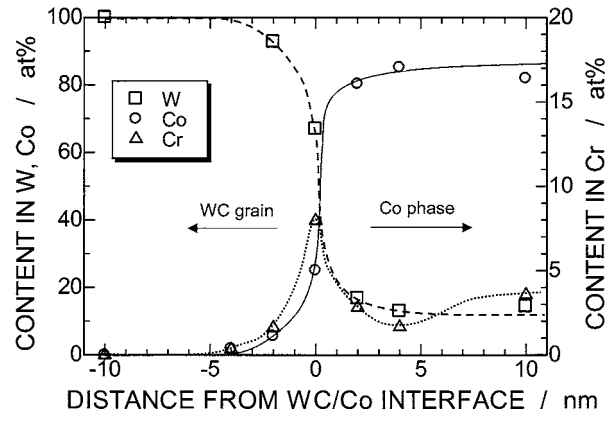

Figure 4 A plot of W, Co and Cr content as a function of distances from the WC/Co interface. Both Cr and Co segregate in the region of less than 4 nm form the interface inside WC grain.

[8, 9]. Jaroenworaluck *et al*. revealed that the morphology of carbide grains drastically changed by a small addition of VC. Typical example of the carbide grains in VC-doped compound is shown in Fig. 5 [4]. In the figure, the WC/Co interface forms multi-steps as indicated by the arrows. From HRTEM and EDS analysis, it was revealed that $(W, V)_2C$ compounds were formed along the fine steps at the WC/Co interface as shown in Fig. 5b. The formation of the compounds was considered to retard the migration of carbide grains. On the contrary, the morphology of carbide grains in Cr-doped compound in the present study is not so different comparing with that of non-doped compound as seen in Fig. 1. Namely the grain growth retardation is not caused by the morphology change of WC/Co interface in the case of Cr-doping. Meanwhile, Okada *et al*. estimated the Cr content in Co-phase to be 5.1at% by electrical leaching technique using ICP analysis for Cr-doped WC-Co compounds [6]. They concluded that the retardation of carbide grains was due to the reduction of the W flux through Co-phase because the solution of Cr reduced W content in Co-phase. However this explanation is not always reasonable because the grain growth is not retarded in WC-Co compounds doped with HfC or ZrC although these dopants can dissolve in Co-phase and reduce the W flux through Co-phase [2]. In the present study, the segregation of Cr was confirmed at WC/Co interface in the Cr-doped WC-Co compounds. The segregation layer would behave like a barrier to retard the process of solution/repreticipation of WC to Co-phase. The details for the retardation mechanism of carbide grains in Cr-doped compound are not still cleared, but this segregation may be considered to play an important role to retard the grain growth.

Fig. 6 is a HRTEM image in the vicinity of WC/WC grain boundary, which corresponds to the b-b interface in Fig. 1b. In the figure, the boundary is set at the edge-on condition and the observation was performed parallel to $[1\bar{2}10]_L$ and $[\bar{1}101]_R$, where subscripts L and R mean the left and the right WC grains in the figure, respectively. The points for EDS analysis are alphabetically indicated in the figure. The boundary is almost parallel to $(0001)_L$ or $(11\bar{2}0)_R$ plane. The boundary is free from any secondary particles or films. It is clear that the two carbide grains are directly contacted in solid state at an atomic level. On the other hand, these carbide grains have the following orientation relationship,

$$(0001)_L//(11\bar{2}0)_R, [1\bar{2}10]_L//[\bar{1}101]_R.$$

The orientation relationship corresponds to special CSL (coincident site lattice) grain boundary, which will be discussed later.

Fig. 7 is EDS spectra taken from the points as indicated in Fig. 6. At the grain boundary, the peak of Cr Kα-line appears while it disappears in the carbide grain. In addition, the presence of Co can be confirmed at the WC/WC boundary in spite of no compounds or films in the HRTEM image. It is thus considered that both Cr and Co segregate at the WC/WC grain boundary although the boundary is essentially stable CSL grain boundary. On the other hand, other WC/WC grain boundaries also exhibit the segregation of Cr and Co.

The grain orientation relationship between adjacent grains has been often discussed in terms of coincidence site lattice (CSL) theory [10]. In the theory, the boundary, which has a special orientation to match adjacent grains geometrically, is classified as a CSL boundary. A type of such boundaries is expressed with Σ-number, which is defined as the ratio of a CSL unit cell volume to a unit cell volume. Generally the Σ numbers have odd values because a half or smaller periodicity exist in the case of even values. However, it was reported by Vicens *et al*. that WC/WC grains has near $\Sigma 2$ relationship. This unique relationship is due to a special a/c ratio of hexagonal WC structure [11]. The a- and c-axis of WC unit cell of $P\bar{6}m2$ is 0.29065 nm

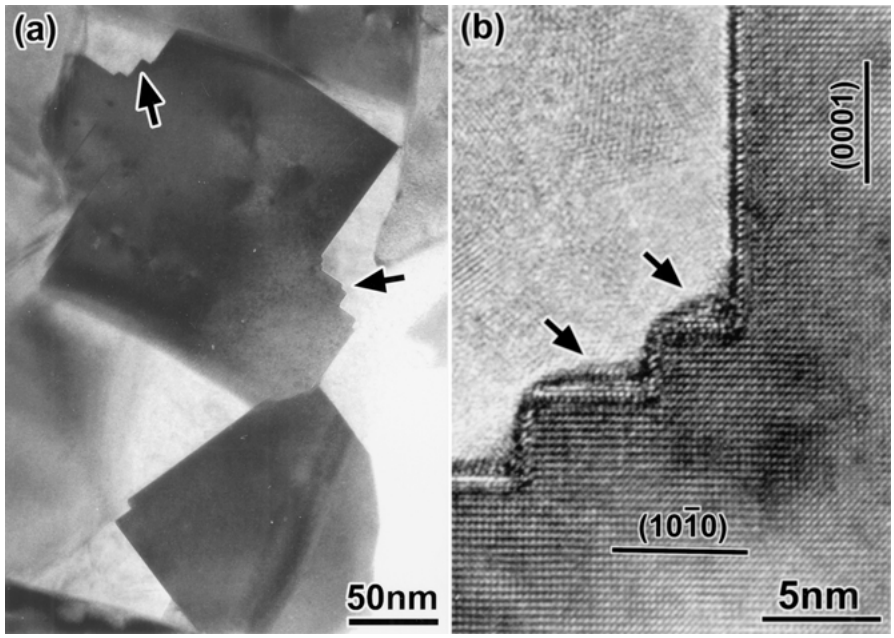

Figure 5 The morphology of WC grain in VC-doped compound, (a) a bright field image and (b) a HRTEM image. Note that fine-multi steps are formed by doping of VC as shown by the arrows.

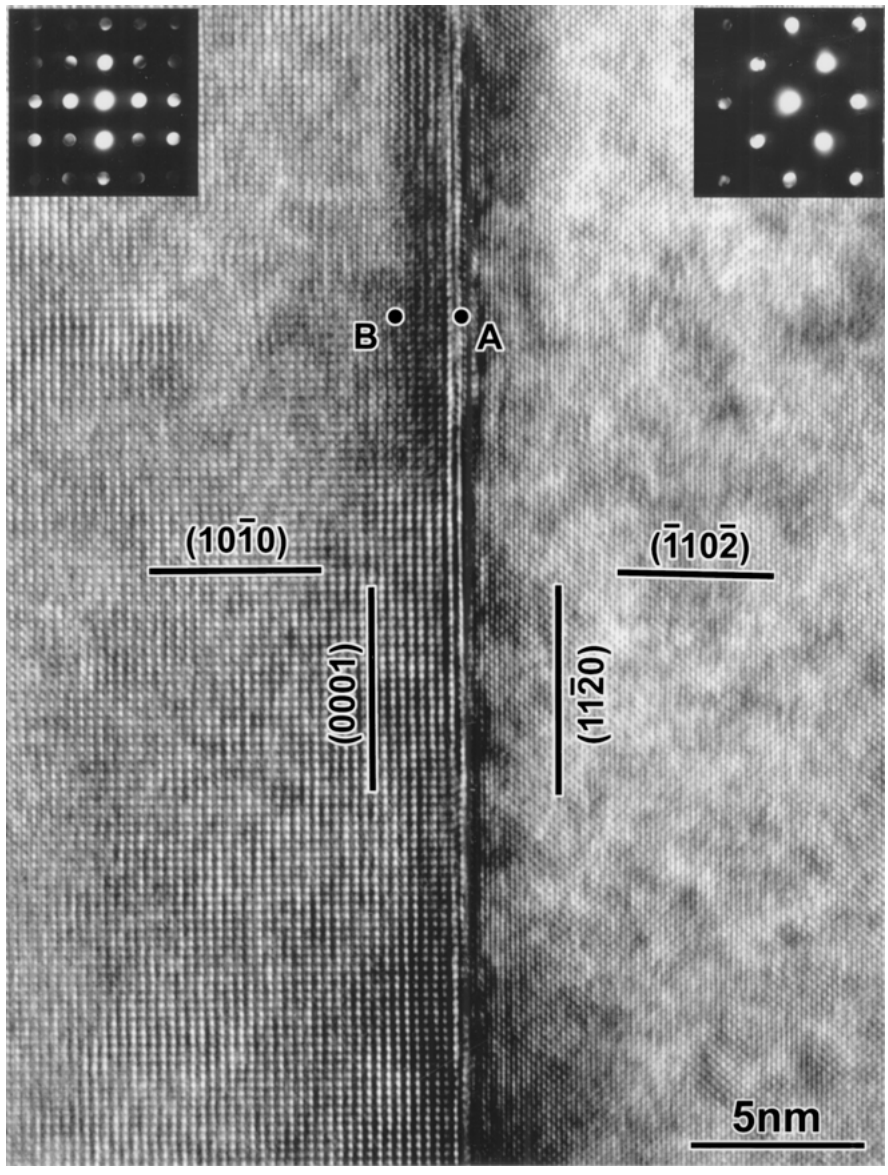

Figure 6 A HRTEM image in the vicinity of WC/WC boundary in the Cr-doped compound. Alphabetical indexes are EDS analysis areas as shown in Fig. 7. The two adjacent WC grains have the following grain orientation relationship, $(0001)_L//(11\bar{2}0)_R$, $[1\bar{2}10]_L//[\bar{1}101]_R$, where the subscriptions L and R are the left and the right grains.

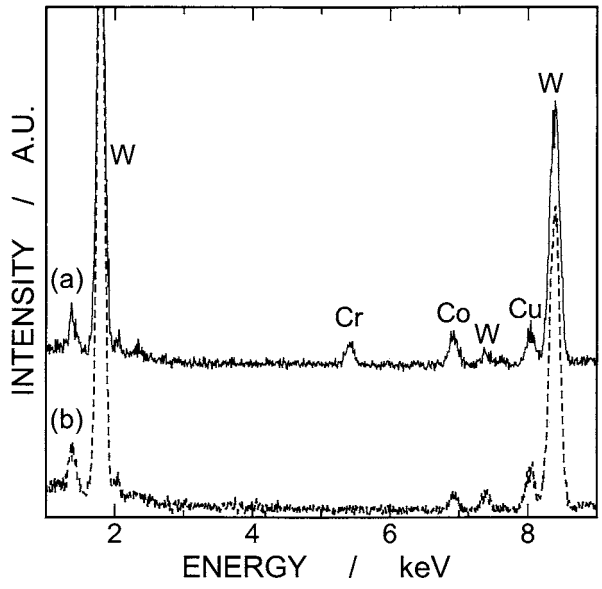

Figure 7 EDS spectra taken from (a) WC/WC boundary and (b) 2 nm away from the boundary. Note that both of Cr and Co segregate at the boundary as seen in (a).

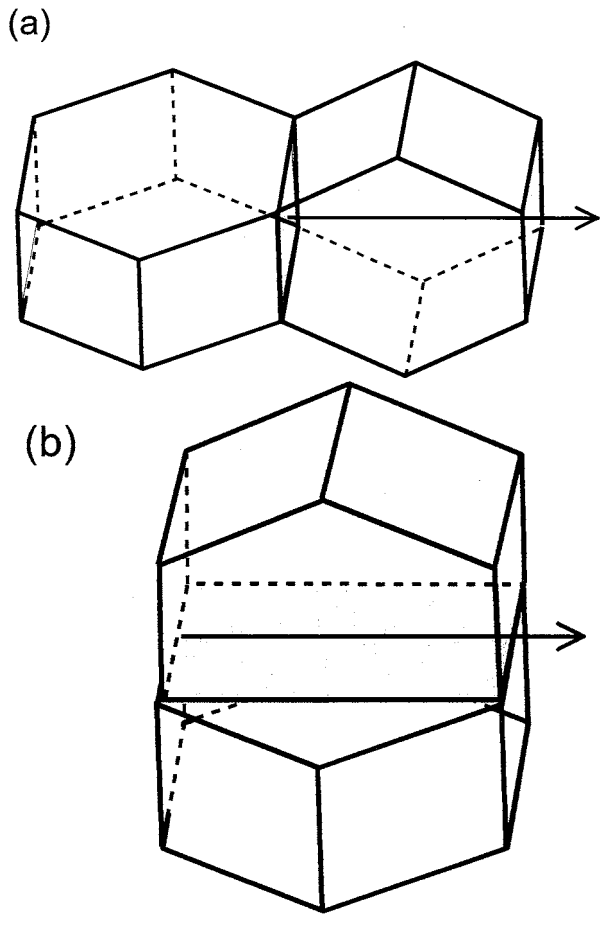

Figure 8 Schematics of the boundaries observed by (a) Vicens *et al*. and (b) this study. The arrows indicate a rotation axis.

and 0.28366 nm respectively so that the a/c-axis ratio has only about 2% mismatch. WC/WC grain boundary observed in this study has the similar grain orientation relationship as Vicens has reported. But the boundary type is different between the two boundaries. Fig. 8 shows schematics of Σ2 WC/WC grains observed by (a) Vicens *et al*., and (b) in this study. The WC/WC boundary observed by Vicens *et al*. is a type of twist boundary as in the figure (a), while the boundary indicated in the figure (b) is an asymmetric tilt type one. These Σ2 grain boundaries are considered to be slightly distorted because of a mismatch of about 2% between a- and c-axis. However, this boundary would be the most stable one because the Σ number is the smallest except Σ1 which has perfectly same orientation relationship. In general, dopants do not tend to segregate at the boundary with low Σ number [12]. But EDS analysis as presented in Fig. 6 clearly showed the co-segregation of Co and Cr at the boundary of Σ2. This may be due to a small distortion caused by a mismatch of about 2%.

4. Conclusions

Microstructure of Cr_3C_2-doped WC-Co was examined by high-resolution electron microscopy and X-ray energy dispersive spectroscopy. The following results were obtained.

1. The addition of Cr_3C_2 was confirmed to reduce carbide grain size.
2. The morphology of WC grains in Cr-doped WC-Co is not so large different from that of non-doped WC-Co. No other compounds can be observed at WC/Co interfaces and WC/WC boundaries.
3. Nano-probe EDS analysis revealed that Co and doped-Cr segregate both at WC/Co interfaces and WC/WC boundaries. In particular, the segregation can be observed even at the asymmetric tilt Σ2 WC/WC boundary.
4. The retardation of carbide grain growth observed in Cr-doped compound is not caused by the morphology change in WC/Co interface. The segregation of Cr and Co at both WC/Co and WC/WC boundaries may be closely related to the retardation.

References

1. J. GURLAND, *Trans. Met. Soc. AIME* **227** (1963) 1146.
2. K. HAYASHI, Y. FUKE and H. SUZUKI, *J. Jpn. Soc. Powder and Powder Metall.* **13** (1972) 67.
3. T. FUKATSU, K. KOBORI and M. UEKI, *Int. J. Refract. Met. & Hard Meter.* **10** (1990) 57.
4. A. JAROENWORALUCK, T. YAMAMOTO, Y. IKUHARA, T. SAKUMA, T. TANIUCHI, K. OKADA and T. TANASE, *J. Mat. Res.* **13** (1998) 2450.
5. *Idem., Ceramic Transactions* **99** (1998) 501.
6. K. OKADA, T. TANIUCHI and T. TANASE, in Proc. Int. Conf. On Powder Metall. & Particulate Mater. 1998, p. 1.
7. J. VICENS, S. LAY, M. BENJDIR and G. NOUET, *Colloque De Physique* **51**C1 (1990) 353.
8. T. TANIUCHI, K. OKADA and T. TANASE, *Proc. 14th Int. Plansee Seminar* **2** (1997) 644.
9. A. EGAMI, M. EHIRA and M. MACHIDA, *Proc. 13th Int. Plansee Seminar* **3** (1993) 639.
10. D. G. BRANDON, *Acta. Metall.* **14** (1996) 1479.
11. J. VICENS, M. BENJDIR and G. NOUET, *J. Mat. Sci.* **29** (1994) 987.
12. T. WATANABE, H. YOSHIDA, T. SAITO, T. YAMAMOTO, Y. IKUHARA and T. SAKUMA, *Materials Science Forum* **304–306** (1999) 601.

Received 31 July 2000
and accepted 30 March 2001